J Therm Anal Calorim (2010) 99:723–731
DOI 10.1007/s10973-009-0616-0

Thermal transitions of polylactide false-twist textured multifilaments determined by DSC and TMA

A. M. Manich · J. Carilla · R. A. L. Miguel · J. M. Lucas · F. G. F. Franco · L. A. Montero · D. Cayuela

MEDICTA2009 Special Issue

Abstract A partially oriented melt-extruded PLA multifilament was false-twist textured to stabilize its structure. Conventional DSC analysis showed a relaxation peak at the end of glass transition. Simultaneous consideration of the TMA curve enabled us to evaluate both the relaxation and the cold crystallisation produced during the DSC scan. The periodic load applied during TMA experiments also enabled us to examine the evolution of Young's modulus along the glass transition, relaxation and cold crystallisation phenomena. Increases in Young's modulus and in enthalpy are related because of crystallisation. Texturing increased crystallinity and decreased cold crystallisation of PLA during the DSC scan.

Keywords Crystallisation · False-twist texturing · Polylactide · Relaxation · Thermal transitions

Introduction

Polylactides (PLA) are biodegradable, biocompatible and hydrolysable aliphatic polyesters, which can be exclusively obtained from renewable resources. Nature-derived lactides are mostly in L-lactide form and exhibit crystalline behaviour. Microstructure, degree of polymerisation and isomer type exert a strong influence on the thermal behaviour (glass transition, crystallisation and melting) of the polymer [1].

The PLA fibre is normally produced by melt extrusion. The effect of draw ratio and draw roll temperature on the orientation, crystallinity and mechanical properties of spun filaments was studied [2], but the influence of subsequent heat setting processes has not been considered to date.

Conventional differential scanning calorimetry (DSC) analysis of PLA filaments shows a peak related to the relaxation of macromolecules in the glass transition region [3]. This can be explained by the tendency of the macromolecules to retract to a more disordered configuration. When the fibre is exposed to a steadily increasing temperature, two transitions, which are due to relaxation/disorientation of the amorphous domains and with crystalline reorganisation such as melting of imperfect crystals and crystallite thickening and perfection, normally appear [4]. At some temperatures, the molecules will obtain enough mobility to spontaneously arrange themselves into a crystalline form. As regards PLA, the glass transition depends on chain flexibility, molecular mass, branching/cross-linking, intermolecular attraction, steric effects and thermal history [5]. It should be noted that PLA is characterised by a glass transition temperature, crystallisation peak and melting peak, typical of semi-crystalline polymers, at about 59, 88 and 164 °C, respectively [6]. A decrease in the storage modulus in the glass transition region is detected at approximately 59 °C using dynamic mechanical analysis (DMA). This is consistent with the results obtained from conventional DSC [7], but no comparison with results given by TMA has been made to date.

A. M. Manich (✉) · J. Carilla
IQAC (Institute of Advanced Chemistry of Catalonia)-CSIC (Spanish National Research Council), Jordi Girona, 18-26, 08034 Barcelona, Spain
e-mail: albert.manich@iqac.csic.es

R. A. L. Miguel · J. M. Lucas · F. G. F. Franco
UBI (Universidade da Beira Interior), Marquês d'Ávila e Bolama, 6201-001 Covilhã, Portugal

L. A. Montero · D. Cayuela
INTEXTER (Textile Research Institute)-UPC (Technical University of Catalonia), Colom, 15, 08222 Terrassa, Spain

The melting behaviour of the PLA fibre detected by DSC does not reflect the melting of original crystallite because of molecular reorganization during heating [8]. Normally, the first peak of the endotherm is attributed to the melting of the original crystals, and the second peak is ascribed to the crystals formed or perfected during the DSC scan [3].

Textile application of PLA requires additional heat-setting of extruded filaments to stabilise them in a particular form. This is carried out by texturing. During this treatment, the flat filament yarn is converted into crimped fibres to simulate the properties of natural staple fibre yarns [9]. In false-twist texturing, the multifilament bundle is cold twisted by running the yarn over the edge of a stack of nine rotating discs on three centres in an equilateral triangle. The yarn runs through the centre of the equilateral triangle and over the edge of each disc. The twisted yarn passes the heater where it is heat plasticized, and twists are heat set in a dry atmosphere close to its melting point. The yarn is subsequently cooled in the area between the heater and the spindle and untwisted after passing the spindle [10]. The two main variables of false-twist texturing that could influence thermal stability of yarn are pre-texturing draw ratio and temperature. As in other semi-crystalline polymers, thermal treatments induce crystallisation on PLA [11].

The combination of thermomechanical analysis and conventional differential scanning calorimetry to study the effect of texturing on relaxation behaviour [12] and on microstructural changes [13] has been successfully used on polyamide 66 filaments and on polyester [14, 15], but it has not been applied up to now on polylactide filaments.

Objective

The aim of this work is to study the effect of false-twist texturing on the thermal stability of polylactide yarns measured by DSC and thermomechanical analysis (TMA). Thermal events detected by DSC can be corroborated by TMA transitions, where variations in yarn length or in storage modulus produced by the periodic load applied are recorded. The relationship between thermal events and texturing variables will also be studied.

Experimental

Materials

Experiments were performed on false-twist textured samples obtained from a melt-extruded partially oriented PLA multifilament 167 dtex/68 POY yarn supplied and textured by ANTEX (Anglès Textil, S.A., 17160 Anglès, Girona, Spain). Texturing conditions were pre-texturing draw ratio and temperature, ranging from 1.3 to 1.4 and from 135° to 165 °C, respectively. Table 1 describes texturing conditions, sample reference of textured yarns, linear density and cross-section. Sample C3 was lost, and values assigned to it were estimated by statistical modelling using the other experimental results.

Methods

Molecular mass

The molecular mass of the polylactide fibres before and after texturation was calculated by viscosimetry in trichloromethane at 25 °C (Ubbelohde viscometer, series 0c). The falling time of the dissolvent (t_0) and those corresponding to five different concentrations c of polymer (t_i) (0.2, 0.4, 0.6, 0.8 and 1.0%, w/w) were determined. For each concentration, the specific viscosity is calculated according to the following equation:

$$\eta_{sp_i} = \frac{t_i - t_0}{t_0}$$

The intrinsic viscosity is obtained from the representation of η_{sp}/c versus c, according to the Huggins equation ($\eta_{sp}/c = [\eta] + k_1[\eta]^2 c$) [16], and the molecular weight of samples in trichloromethane at 25 °C was calculated by applying the Mark-Houwink equation [17]:

$$[\eta] = 5.45 \cdot 10^{-4} \cdot \overline{M_n}^{0.73}$$

Tensile properties of the multifilaments

Ten specimens with gauge length of 100 mm were tested after being conditioned in a standard atmosphere for 48 h.

Table 1 Texturing conditions (draw ratio and temperature) of PLA 167dtex/68 multifilament, sample reference, linear density and estimated cross-section through PLA density (1.25 g cm^{-3})

Draw ratio/v_1/v_0	1.30			1.35			1.40		
Temperature/°C	135	150	165	135	150	165	135	150	165
Reference	*A1*	*A2*	*A3*	*B1*	*B2*	*B3*	*C1*	*C2*	*C3**
Yarn linear density/dtex	224.1	221.1	218.0	216.3	213.9	213.6	210.9	206.9	205.4
Cross-section/mm^2 × 1000	17.93	17.69	17.44	17.30	17.11	17.09	16.87	16.55	16.43

Remark: Results of sample C3 were estimated through the best fitted model

Breaking stress and strain were determined on specimens subjected to tensile testing at 60% min^{-1} according to the ASTM D2101 Standard [18].

Differential scanning calorimetry

Glass transition, relaxation, cold crystallisation and melting events were determined by a Mettler Toledo DSC-823 apparatus. Textured filaments were cut in very short lengths, and duplicated samples of approximately 6 mg were sealed in 40 µl aluminium punched pans to guarantee good contact of the sample with the DSC sensor. Replicated DSC curves were obtained under the following operating conditions: Initial temperature 30 °C, final temperature 200 °C, heating rate 10 °C min^{-1} and nitrogen purging gas 35 ml min^{-1}. The DSC curves resembled the plot in Fig. 1.

The following parameters were determined from the DSC curve:

T_g/°C: Onset temperature of the first endothermic relaxation peak.
T_{rp}/°C: Peak temperature of relaxation.
ΔH_r/J g^{-1}: Relaxation enthalpy.
T_{cco}/°C: Onset temperature of cold crystallisation.
ΔH_{cc}/J g^{-1}: Enthalpy of cold crystallisation.
ΔH_m/J g^{-1}: Melting enthalpy.

The percentage of crystallinity X was calculated by comparing the difference between melting and crystallisation enthalpies with the melting enthalpy of a 100% crystalline PLA sample [19] that is 93.7 J g^{-1}, through the relationship $100 \times (\Delta H_m - \Delta H_{cc})/93.7$ [20].

Thermomechanical analysis

Two samples of each reference (Table 1) 12.8 mm in length were tested in a TMA/SDTA 840 Mettler Toledo at three different periodic loads under the following conditions: Initial temperature 25 °C, final temperature 165 °C, heating rate 10 °C min^{-1}, nitrogen purging gas 35 mL min^{-1} and 1/12 Hz periodic loads between 0.025 and 0.05 N, 0.05 and 0.10 N, and 0.1 and 0.2 N. Variations in length given by TMA resembled those in Fig. 2. The deformation amplitude is inversely related to Young's modulus. The following parameters were determined [15] by analysing the mean curve of the variations in length and the E-storage modulus with temperature.

Variation in length of mean curve:

T_{So}/°C: Onset temperature of shrinkage.
T_{Sp}/°C: Peak temperature of shrinkage.
S_r/%: Relaxation shrinkage at T_{Sp}.
T_{Se}/°C: Endset temperature of shrinkage.

E-storage modulus curve (see Fig. 3):

E_o/MPa: Initial storage modulus before glass transition.

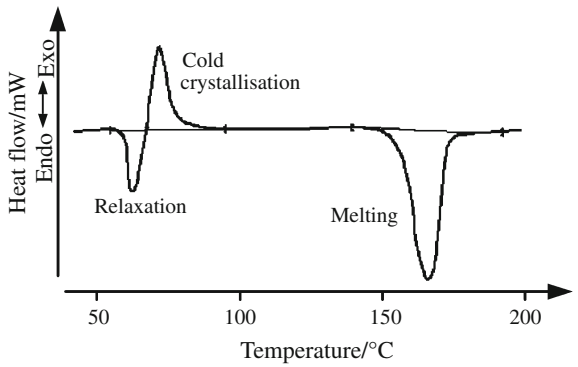

Fig. 1 DSC curve of PLA false-twist textured multifilament from 30 to 200 °C at 10 °C min^{-1}

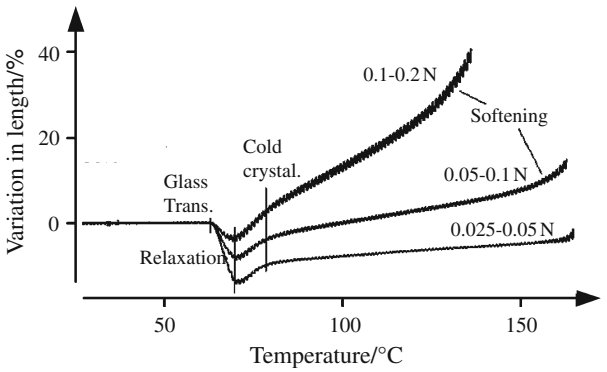

Fig. 2 TMA curves of PLA false-twist textured multifilaments 12.8 mm in length at three different periodic loads applied at 1/12 Hz (0.025–0.050 N, 0.05–0.10 N and 0.1–0.2 N), from 25 to 165 °C at 10 °C min^{-1}

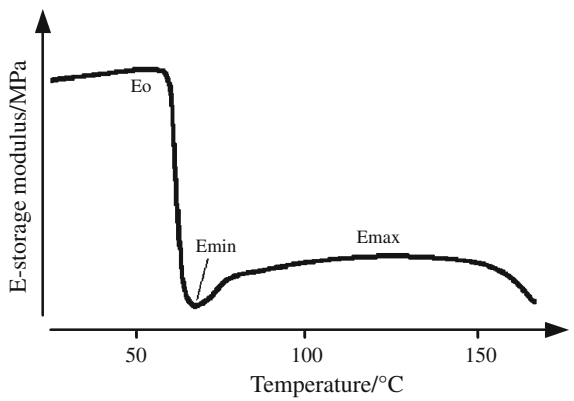

Fig. 3 Evolution of the E-Storage modulus curve of PLA false-twist textured multifilament 12.8 mm in length from 25 to 165 °C at 10 °C min^{-1} subjected to a periodic load between 0.025 and 0.05 N at 1/12 Hz

T_{Einf}/°C: Temperature at the inflection point of the E-storage modulus fall curve.
E_{slope}/MPa K^{-1}: Relaxation slope of the E-storage curve at T_{Einf}.
E_{min}/MPa: Minimum E-storage modulus after glass transition and relaxation.
T_{Emin}/°C: Temperature at which E_{min} is observed.
T_{φ}/°C: Temperature of maximum phase lag between E-storage and E-loss.
E_{max}/MPa: Maximum storage modulus after cold crystallisation.

Statistical analysis

Experiments were designed according to a 3-level factorial design including the following variables: pre-texturing draw ratio x_1, texturing temperature x_2 and, in TMA trials, the mean testing periodic load x_3. Therefore, the influence of the variables on each response y can be analysed by fitting empirical model $y = b_o + \Sigma_i\ b_i\ x_i + \Sigma_{ij}\ b_{ij}\ x_i\ x_j$ using regression analysis. The application of the Analysis of Variance [21] enabled us to remove the non-significant variables from the model to obtain the 'best' regression equation [22]. The responses that would correspond to sample C3 were estimated by the application of the 'best' model. Statistical software [23] was used to perform the analysis.

Results and discussion

Molecular mass and mechanical properties

The effect of texturing on the molecular mass and mechanical properties of the polylactide multifilaments was measured by comparing the values of the original POY yarn with those obtained after texturing according to Table 1. Texturing decreased the molecular mass from 38.9 ± 0.3 kg mol^{-1} to a mean value of 32.5 ± 0.2 kg mol^{-1} for textured yarns in accordance with its poor resistance to hydrolysis [24]. As regards the mechanical properties, texturing increased breaking stress from 18.2 ± 0.7 cN tex^{-1} to a mean value of 23.3 ± 0.4 cN tex^{-1}. The best result was the one reached by sample B2 textured at 150 °C with a previous draw of 1.35 (see Table 2). Texturing decreased breaking strain from 74.7 ± 4.1% to a mean value of 35.6 ± 1.2%. The higher the draw ratio, the lower the breaking strain: an increase in draw ratio from 1.3 to 1.4 produces a decrease of 6% in breaking strain due to the improved orientation of the macromolecules in the filament. When the texturing temperature rises from 135 to 165 °C, the breaking strain is increased by 2.85%. The decrease in molecular mass is offset by the increase in both orientation and crystal perfection, resulting in filaments with higher stress and lower strain those of the original non-textured filament at breaking.

Differential scanning calorimetry and thermomechanical analysis

The mean values of replicated tests obtained by DSC and TMA at three periodic testing loads are shown in Tables 3 and 4, respectively, which include the mean value of the replicates and the pooled standard deviation of the results. Comparison of both techniques offers some insights into the relaxation and cold crystallisation processes during the DSC scan.

Table 3 Mean values of the results given by DSC according to the reference

Reference	T_g/°C	T_{rp}/°C	ΔH_r/Jg^{-1}	T_{cco}/°C	ΔH_{cc}/Jg^{-1}	ΔH_m/Jg^{-1}	X/%
A1	64.8	70.5	7.74	69.8	14.35	43.29	30.9
A2	65.0	70.9	7.65	69.6	13.92	45.35	33.5
A3	64.8	71.7	5.43	69.4	10.29	44.21	36.2
B1	64.8	70.8	7.89	69.7	13.89	42.48	30.5
B2	64.9	71.6	6.51	69.5	11.55	44.56	35.2
B3	64.9	72.6	4.06	69.3	9.08	43.17	36.4
C1	64.6	71.5	5.81	68.8	11.68	44.23	34.7
C2	64.7	72.4	5.05	68.6	10.11	44.12	36.3
C3*	64.7	72.8	1.73	68.4	7.32	43.47	38.6
SD	±0.2	±0.5	±0.54	±0.3	±0.84	±1.05	±0.9

Remarks: *Results of sample C3 were estimated through the best fit model

Glass transition temperature T_g, peak temperature T_{rp} and enthalpy ΔH_r of relaxation, onset temperature T_{cco} and enthalpy ΔH_{cc} of cold crystallisation, melting enthalpy ΔH_m and initial crystallinity X of the PLA textured multifilaments. The pooled standard deviations SD estimated with 8 degrees of freedom are included

Table 2 Mean values of breaking stress and strain (±SD standard deviation) of the polylactide textured multifilaments according to the references in Table 1

Reference	A1	A2	A3	B1	B2	B3	C1	C2
Stress/cN tex^{-1}	22.1 ± 0.8	23.3 ± 0.6	23.3 ± 0.5	23.4 ± 0.6	25.2 ± 0.5	24.2 ± 1.1	21.2 ± 0.6	23.8 ± 0.5
Strain/%	37.5 ± 2.6	38.0 ± 1.6	40.6 ± 1.2	34.5 ± 1.6	35.7 ± 1.4	36.2 ± 2.7	29.6 ± 1.1	32.8 ± 1.0

Table 4 Mean values of the results given by TMA according to the reference and testing periodic load at 1/12 Hz

Ref	T_{So}/°C	T_{Sp}/°C	S_r/%	T_{Se}/°C	E_o/MPa	T_{Einf}/°C	E_{slope}/MPaK^{-1}	E_{min}/MPa	T_{Emin}/°C	T_φ/°C	E_{max}/MPa
Periodic load between 0.025 and 0.050 N											
A1	64.8	70.5	18.0	77.8	1731	65.0	431.0	25.9	69.2	67.5	423.4
A2	65.0	70.9	15.0	78.6	1649	64.9	401.4	34.1	69.7	67.8	380.8
A3	64.8	71.7	11.5	80.1	1675	65.0	279.9	75.0	70.4	68.5	386.3
B1	64.8	70.8	15.7	78.4	1523	65.2	393.9	34.1	69.5	68.1	396.4
B2	64.9	71.6	13.2	80.2	1839	64.8	343.3	61.6	70.3	68.5	384.7
B3	64.9	72.6	10.4	82.0	1843	66.1	282.0	119.3	71.3	68.7	391.2
C1	64.6	71.5	13.3	79.8	1549	64.8	313.4	61.0	70.2	68.7	415.3
C2	64.7	72.4	11.4	82.0	1689	65.4	239.4	106.2	71.2	69.0	409.0
C3*	64.7	72.8	8.7	84.8	1687	66.7	155.0	167.1	71.8	70.0	410.5
SD	±0.2	±0.7	±2.5	±1.7	±239	±0.5	±109.5	±33.5	±0.7	±0.5	±17.8
Periodic load between 0.05 and 0.10 N											
A1	65.0	70.8	8.3	78.7	2560	65.0	642.7	95.6	70.4	67.7	362.3
A2	65.1	71.1	8.1	79.8	2825	64.9	616.2	107.8	70.5	67.7	359.5
A3	65.3	71.7	6.6	81.8	2465	65.4	342.7	160.9	71.4	68.7	382.7
B1	65.1	71.0	8.0	79.5	2726	64.9	548.1	121.1	70.7	67.7	367.8
B2	65.2	71.6	7.6	80.1	2629	64.9	428.3	149.0	71.3	68.2	369.5
B3	65.5	72.2	6.2	84.6	2282	65.9	332.1	211.5	71.9	69.1	369.9
C1	64.9	71.5	7.7	79.9	2809	64.8	462.7	170.6	71.3	69.0	384.2
C2	65.3	72.0	6.7	81.1	2649	65.9	383.0	209.9	71.9	69.2	387.7
C3*	65.4	72.8	5.0	84.6	2618	66.5	290.2	263.8	72.7	70.0	385.1
SD	±0.2	±0.5	±0.8	±1.8	±228	±0.5	±122.1	±42.4	±0.6	±0.7	±11.9
Periodic load between 0.10 and 0.20 N											
A1	64.7	69.0	2.3	79.6	3297	64.7	476.0	219.4	71.3	68.0	356.5
A2	65.0	70.0	2.7	80.7	3254	64.8	463.5	220.4	71.7	67.6	343.8
A3	65.1	70.1	2.2	82.3	3104	64.8	352.3	265.9	72.4	68.6	350.4
B1	64.9	69.2	3.2	79.7	3691	64.8	530.1	254.1	71.9	67.6	374.3
B2	65.1	70.1	2.9	80.7	2976	64.8	447.1	293.7	72.3	68.5	403.9
B3	65.5	71.1	2.1	83.6	3243	65.7	306.9	331.2	73.1	69.4	393.7
C1	65.2	70.5	3.0	80.3	3238	64.8	365.1	298.0	72.8	69.8	391.7
C2	65.3	70.0	1.4	80.5	3023	64.9	298.6	301.0	72.5	69.1	370.5
C3*	65.6	71.3	2.4	84.5	3228	66.4	225.7	391.5	73.5	70.0	385.1
SD	±0.3	±0.7	±0.7	±1.4	±381	±0.5	±87.8	±40.0	±0.6	±0.9	±24.8

Remark: Results of sample C3 were estimated through the best fit model

Onset T_{So} and peak T_{Sp} temperatures of shrinkage, relaxation shrinkage Sr and endset temperature T_{Se} of shrinkage. Initial storage modulus E_o, inflection temperature T_{Einf} and slope E_{slope} of E-storage, minimum E-storage E_{min} and temperature T_{Emin}, temperature of maximum phase lag T_φ, and maximum E-storage after crystallisation E_{max}. The pooled standard deviations SD estimated with 8 degrees of freedom for each periodic load are included

Glass transition and macromolecular relaxation

The first thermal event detected by DSC is glass transition, followed by a relaxation peak. The estimated T_g is about 62.5 °C regardless of the texturing variables. The peak temperature of relaxation is about 66 °C, with a slight influence of the texturing temperature. The enthalpy of relaxation is significantly influenced by texturing variables and decreases with the increase in the texturing effect as shown in Fig. 4. The effect of texturing temperature on the enthalpy of relaxation was higher than that of the draw ratio. The relaxation process lasts up to approximately 69 °C, when the mobility of the macromolecules in the amorphous phase is monotonously increased with increasing temperature.

When the same relaxation process is observed by means of the mean dilatation curve provided by TMA, the start of the relaxation process is estimated by the onset temperature of shrinkage T_{So} of about 65 °C. This temperature is 2.5 °C higher than T_g measured by DSC, probably due to the

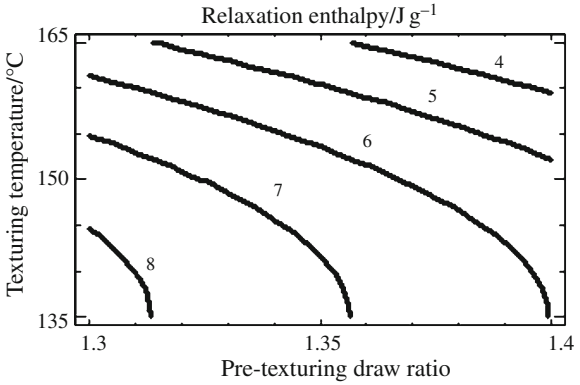

Fig. 4 Evolution of the relaxation enthalpy of PLA false-twist textured filaments measured by DSC above glass transition

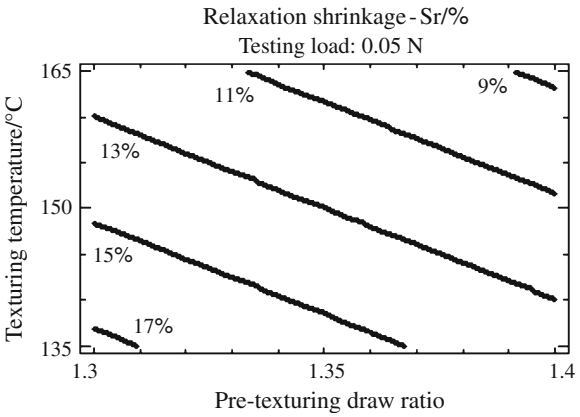

Fig. 5 Evolution of the maximum relaxation shrinkage of PLA false-twist textured filaments measured by the TMA at 1/12 Hz periodic loads between 0.025 and 0.050 N

effect of the applied load. Very slight influences of testing load and texturing temperature on T_{So} were detected.

The effects of texturing variables on the relaxation shrinkage S_r were in line with the effect of these variables on the relaxation enthalpy measured by DSC (see Fig. 5). There is consequently a good linear relationship between both variables: the enthalpy of relaxation and the relaxation shrinkage. The best relationship was obtained with the lowest load testing level ($r = 0.98$).

The peak temperature of shrinkage T_{Sp} indicates the end of the relaxation process when the polymer attains its highest entropic state. T_{Sp} ranged from 69 to 71 °C depending on the testing load. This temperature was slightly increased by the intensity of texturing in a way similar to that observed by the relaxation shrinkage in Fig. 5. T_{Sp} attains values close to that which marks the end of the relaxation process measured by DSC.

As regards the evolution of the E-storage modulus, the glass transition temperature was assessed by the inflection point of the marked fall in the E-storage curve T_{Einf}, where the biggest change (fall) in the modulus occurs [25]. T_{Einf} was about 65–66 °C, which was very close to T_{So} and between T_g and T_{rp} detected by DSC. The delay in detecting the glass transition can be attributed to the effect of the testing load, which hinders the relaxation process.

The intensity of relaxation can be estimated by the decrease in the E-storage modulus from the highest initial value E_o before glass transition to the lowest value after relaxation E_{min} measured in percentage $100 \times (E_o - E_{min})/E_{min}$, and by the slope of the E-storage curve E_{slope} at the inflection point. Both values decrease with the intensity of texturing following tendencies similar to that of the relaxation enthalpy (Fig. 4). Consequently, it may be assumed that all these responses estimate the intensity of the relaxation effect after T_g. The best correlations were those obtained between relaxation enthalpy and E_{slope} ($r = 0.95$), and between the decrease in the E-storage modulus and relaxation shrinkage ($r = 0.97$) at the low level of testing load.

The region of glass transition is evidenced by the rapid decrease in the E-storage modulus and by the upward contribution of the E-loss modulus because of the increasing mobility of macromolecules in the amorphous phase, resulting in a maximum phase lag between the E-storage and the E-loss moduli. The temperature of maximum phase lag T_φ ranged from 68 to 69.5 °C, when the maximum contribution of the amorphous phase was attained although the applied load in TMA hindered the relaxation process. T_φ was slightly increased by the intensity of the texturing effect.

The relaxation process is marked by the dissociation of the cross-link bonds in the amorphous phase, which reduces its contribution to stress. The situation is defined by a minimum in the E-storage modulus which occurs between 69.5 and 71.5 °C when measured at the lowest loading. This value is significantly affected by the texturing variables. This temperature was slightly higher than that obtained by DSC due to the restrictions imposed by the testing load.

Cold crystallisation during the DSC scan

At approximately 69 °C, the PLA macromolecules attain their maximum freedom of inter-chain mobility. This facilitates their spontaneous arrangement into different crystal forms, giving rise to a cold crystallisation process that is prolonged from 6 to 10 °C. It may be observed that both the temperature range and the enthalpy of cold crystallisation decrease with the intensity of texturing, especially with texturing temperature. This may be ascribed to the higher level of previous recrystallisation induced by texturing. Figure 6 shows the effect of texturing variables on cold crystallisation enthalpy.

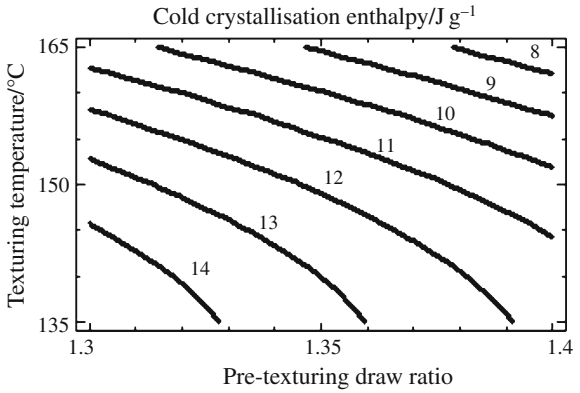

Fig. 6 Evolution of the cold crystallisation enthalpy of PLA false-twist textured filaments according to texturing variables measured by DSC

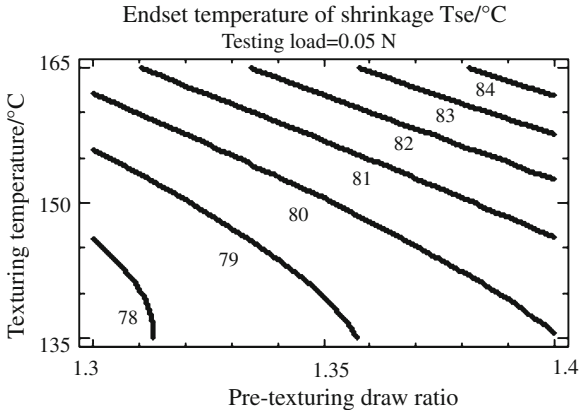

Fig. 8 Endset temperature of shrinkage Tse measured on the dilatation curve of TMA at 0.025–0.05 N of periodic load at 1/12 Hz, which match the endset temperature of cold crystallisation during DSC scan

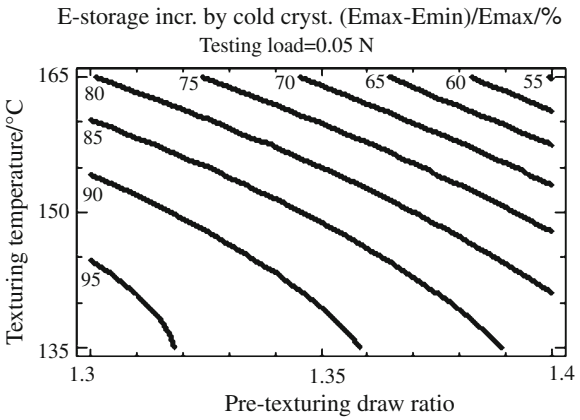

Fig. 7 Increase in the E-storage modulus due to cold crystallisation of PLA false-twist textured filaments during DSC scan, measured by TMA at 0.025–0.05 N of periodic load at 1/12 Hz

During the cold crystallisation process, recrystallisation not only occurs but crystal size and perfection [4] play a major role in the increase in the E-storage modulus of the filament, which attains a new maximum E_{max}. The evolution of this parameter measured by the TMA at low testing load, in percentage, is shown in Fig. 7. It should be noted that there is a perfect linear correlation between the cold crystallisation enthalpy and the increase in the E-storage modulus ($r = 0.98$), which demonstrates that both parameters reflect the same phenomenon of cold crystallisation.

The parameter that best indicates the end of the cold crystallisation process is the endset temperature of shrinkage T_{Se}, when a sudden decrease in the slope of the dilatation mean curve can be observed. This confirms that a higher level of crystallisation has been attained. Figure 8 shows the evolution of T_{Se} measured by TMA at the lowest testing load as a function of the texturing variables.

Crystallinity induced by false-twist texturing

The efficiency of heat-setting induced by texturing depends on the freedom of molecular mobility and on the opportunity for crystal melting with re-crystallisation [26]. The initial percentage of crystallinity of PLA filaments before texturing was calculated by the difference between melting and cold crystallisation enthalpies provided by the DSC scan divided by the melting enthalpy of a 100% crystalline PLA sample. The initial crystallinity of the PLA multifilament was 24.3%. Figure 9 shows the evolution of crystallinity of false-twist textured PLA multifilaments according to texturing conditions. Texturing increases crystallinity from 27 to 60% with respect to the original crystallinity. Variations in pre-texturing draw ratio from 1.3 to 1.4 lead to an increase of 12% in crystallinity, while an increment from 135 to 165 °C in texturing temperature enables the crystallinity to rise by 20%.

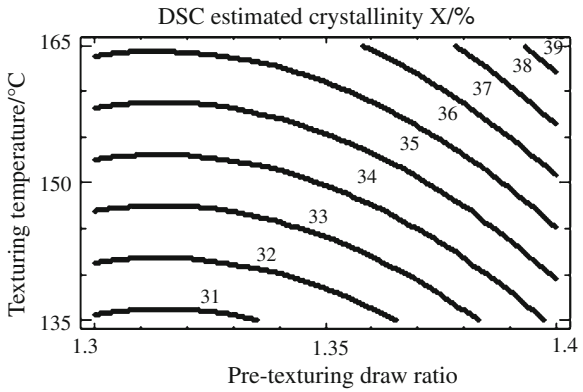

Fig. 9 Crystallinity X of the false-twist textured PLA multifilaments measured by comparison of melting and cold crystallisation enthalpies given by the DSC

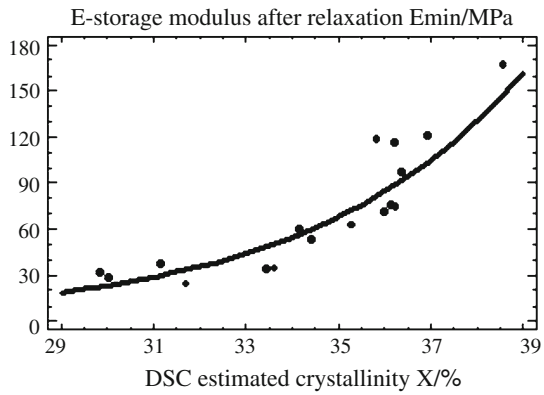

Fig. 10 Relationship between crystallinity and the E-storage modulus after relaxation measured at low testing load of the false-twist textured PLA multifilaments

It is well known that, after relaxation, mainly the macromolecules in the crystalline phase determine the mechanical properties of the filaments. Therefore, the E-storage modulus after relaxation, E_{min}, should be related to the original crystallinity X of the textured filaments. Figure 10 shows the upward relationship between both variables. The higher the crystallinity, the greater the impact on the increase in the E-storage modulus.

Conclusions

In the light of our findings, the following conclusions may be drawn:

- False-twist texturing of PLA melt-spun multifilaments increase crystallinity from 27 to 60%.
- The effect of texturing temperature on the induced recrystallisation of the multifilaments is stronger than that of the pre-texturing draw ratio.
- When the sample is subjected to increasing temperatures, after glass transition, a relaxation process is observed up to 69 °C. At this temperature, the mobility of the macromolecules is increased, favouring cold crystallisation prolonged from 6 to 10 °C.
- The intensity of relaxation and cold crystallisation processes can be evaluated by the enthalpies provided by DSC or by the variations in the E-storage modulus yielded by TMA, which show a good correlation between them.

Acknowledgements The authors are indebted to the Spanish MAT2007-66569-C02-02 Project, and to Anglès Textil S.A. (ANTEX) for the manufacturing process of samples. Thanks are also due to Ms. A. Lopez and C. Ferrero for their assistance in the experimental work, and to Mr. George von Knorring for improving the final version of the manuscript.

References

1. Ahmed J, Zhang JX, Song Z, Varshney SK. Thermal Properties of Polylactides. Effect of molecular mass and nature of lactide isomer. J Therm Anal Calorim. 2009;95:957–64.
2. Solarski S, Ferreira M, Devaux E. Thermal and mechanical characteristics of polylactide filaments drawn at different temperatures. J Text Inst. 2007;98:227–36.
3. Solarski S, Ferreira M, Devaux E. Characterization of the thermal properties of PLA fibers by modulated differential scanning calorimetry. Polymer. 2005;46:11187–92.
4. Buchanan DR. Thermomechanical responses of fibres. In: Mukhopadhyay SK, editor. Advances in fibre science. Manchester: The Textile Institute; 1992. p. 87–112.
5. Chow WS, Lok SK. Thermal properties of poly(lactic acid)/organo-mont-morillonite nanocomposites. J Therm Anal Calorim. 2009;95:627–32.
6. Mojumdar SC, Sain M, Prasad RC, Sun L, Venart JES. Selected thermoanalytical methods and their applications from medicine to construction. J Therm Anal Calorim. 2007;90:653–62.
7. Malmgren T, Mays J, Pyda M. Characterization of poly(lactic acid) by size exclusion chromatography, differential refractometry, light scattering and thermal analysis. J Therm Anal Calorim. 2006;83:35–40.
8. Mogi K, Kubokawa H, Hatakeyama T. Effect of dyeing on melting behaviour of poly(lactic acid) fabric. J Therm Anal Calorim. 2002;70:867–75.
9. Manich AM, Maíllo J, Cayuela D, Carilla J, Ussman M, Gacén J. Effect of the air-jet and the false-twist texturing processes on the thermomechanical behaviour of polyamide 6.6 yarns. J Therm Anal Calorim. 2008;93:921–6.
10. Foster PW, Mukhopadhyay SK, Jeetah R, Porat I, Greenwood K. Constant-bulk false-twist texturing. Part I: principle and method. J Text Inst. 1992;83:414–22.
11. Day M, Nawaby AV, Liao X. A DSC study of the crystallization behaviour of polylactid acid and its nanocomposites. J Therm Anal Calorim. 2006;86:623–9.
12. Manich AM, Maíllo J, Cayuela D, Gacén J, de Castellar MD, Ussman M. The effects of texturing induced microstructural changes on the relaxation behaviour of polyamide 66 multifilament yarns. Fiber Polym. 2007;8:512–9.
13. Manich AM, Maíllo J, Cayuela D, Gacén J, de Castellar MD, Ussman M. Heatsetting, microstructural changes and thermomechanical behaviour of polyamide 66. In: Krucińska I, Zajączkowski J, editors. Proceedings of the IX international scientific conference IMTEX 2007. Łódź Poland; 2007. pp. 82–86.
14. Cayuela D, Manich AM, Gacén I, Gacén J. Determination of the heatsetting temperature of polyester by TMA. J Therm Anal Calorim. 2003;72:729–35.
15. Manich AM, Bosch T, Carilla J, Ussman MH, Maíllo J, Gacén J. Thermal analysis and differential solubility of polyester fibers and yarns. Text Res J. 2003;73:333–8.
16. Huggins ML. The viscosity of dilute solutions of long-chain molecules. IV. Dependence on concentration. J Am Chem Soc. 1942;64:2716–8.
17. Peesan M, Rujiravanit R, Supaphol P. Electrospinning of hexanoyl chitosan/polylactide blends. J Biomater Sci Polym Ed. 2006;17:547–65.
18. Standard Test Method ASTM D 2101. Tensile properties of single man-made textile fibres taken from Yarns and Tows; 1979.
19. Jaffe M, Menczel JD, Bessey WE. Fibers. In: Turi EA, editor. Thermal characterization of polymeric materials. London: Academic; 1981. p. 1928.

20. Cayuela D, Gacén J. Contribution of the secondary crystallization to the overall crystallinity of heatset polyester. J Therm Anal Calorim. 1994;41:1599–605.
21. Montgomery DC. Design and analysis of experiments. 5th ed. New York: Wiley; 2001.
22. Draper NR, Smith H. Applied regression analysis. 2nd ed. New York: Wiley; 1981.
23. Statgraphics 5 Plus. Manugistics, Inc. 2115 Jefferson street, Rockwille, Maryland 20852, USA.
24. Farrington DW, Lunt J, Davies S, Blackburn RS. Poly(lactic acid) fibers. In: Blackburn RS, editor. Biodegradable and sustainable fibres. Cambridge: Woodhead Publishing Ltd; 2005. p. 191–219.
25. Ward IM, Hadley DW. An introduction to the mechanical properties of solid polymers. Chichester: Wiley; 1993.
26. Mukhopadhyay SK. Nature and mechanisms of heat-setting of fibres. In: Mukhopadhyay SK, editor. Advances in fibre science. Manchester: The Textile Institute; 1992. p. 115–38.